



High absorbency cellulose acetate electrospun nanofibers for feminine hygiene application

Shital Yadav, Mani Pujitha Illa, Tulika Rastogi, Chandra Shekhar Sharma*

Department of Chemical Engineering, Indian Institute of Technology, Hyderabad, Kandi 502285, Telangana, India

ARTICLE INFO

Article history:

Received 5 May 2016

Received in revised form 30 June 2016

Accepted 13 July 2016

Keywords:

Electrospinning

Cellulose acetate

Nanofibers

Superabsorbent polymers

Feminine sanitary napkins

ABSTRACT

The feminine sanitary napkin is an important disposable absorbent hygiene product. Superabsorbent polymers (SAPs) are added in the absorbent core of sanitary napkins in order to improve their absorption capacity. However, they are found to have certain adverse effects on the health of user and also on the environment. Here, we demonstrate the potential use of electrospun cellulose acetate (CA) nanofibers as a material for absorbent core in feminine sanitary napkins. The analysis in terms of morphology, surface area, porosity, strength, absorption capacity, and percentage residue was done and further compared with some of the known commercially available feminine sanitary napkins. Considering the large surface area and porosity, it is found that the electrospun nanofibers provide a better alternative to achieve even higher absorbency that too without adding SAP. Sanitary napkins without SAP can be a solution for its safe disposal, and therefore, can have global impact in the near future.

© 2016 Elsevier Ltd. All rights reserved.

1. Introduction

Menstrual hygiene is an important issue for every woman, as poor menstrual hygiene increases the vulnerability toward reproductive tract infections (RTIs) [1]. There are different types of feminine hygiene products commercially available, such as sanitary napkins, tampons, panty shields, wipes, and cosmetic removal pads. Among these, feminine sanitary pad/napkin is an important disposable absorbent hygiene product. Its functions are to absorb and retain menstrual fluid discharge and isolate it from skin, along with maintaining comfort, preventing odor, and staying in place [2]. To accomplish all these requirements, sanitary pads constitute different layers like cover stock, acquisition and distribution layer, absorbent core, back sheet, tissue, elastic wing, and siliconized paper [2]. Absorbent core gives the desired absorption capacity to sanitary pads and is mainly made up of hydrophilic cellulosic fibers such as wood-derived fluff pulp or viscose rayon [2]. As the diameter of these cellulosic fibers present in commercially available products is in the range of few tens of microns, their absorption capacity is less owing to their lower surface area. To improve the absorption capacity, some of the commercially available feminine hygiene products use superabsorbent polymers (SAPs) either in the form of granules within cellulosic fiber matrix or in the form of composite fabric layer [2].

SAPs are commonly divided into two main classes, i.e., synthetic (petrochemical-based) and natural (polysaccharide- and polypeptide based) [3]. Most of these superabsorbents are produced from acrylic acid, its salt, and acrylamide [3]. The superabsorbents available in the market today are primarily based on cross-linked sodium polyacrylate (SPA) gels [2]. It facilitates in increasing the liquid absorption capacity and liquid retention capacity tremendously, thus allowing the product to be thinner with improved performance [2].

However, there are some harmful chemicals present in the commercially available sanitary napkins. For example, dioxins are used to bleach the cotton/material used for making absorbent core, and it is responsible for side effects in the body such as pelvic inflammatory disease, ovarian cancer, immune system damage, impaired fertility and diabetes [4]. As mentioned above, SAPs are added to increase the absorption capacity, but in 1980s, use of SAPs was restricted in tampons due to its possible link with toxic shock syndrome, a potentially fatal illness caused by a bacterial toxin [5]. Further, as SAPs are petroleum-based products and therefore do not degrade readily in landfills, their use is not eco-friendly as well.

Therefore, the objective of this work is to minimize the use of SAPs in feminine hygiene products considering their possible adverse health effects. For this, we intend to fabricate cellulose-based nanofibers and suggest their use as absorbent core in feminine hygiene products. The increased specific surface area of nanofibers as compared to micron-sized fibers present in commercial products also justifies well this objective and may compensate for the absorption capacity achieved by using SAPs.

* Corresponding author.

E-mail address: cssharma@iith.ac.in (C.S. Sharma).

Electrospinning is one of the simple and cost-effective method used to synthesize fibers with diameter ranging from 10 nm to 10 μm [6,7]. This method was invented by Formhals in 1934 [8]. Electrospinning process uses high electric field as a driving force to draw fibers from electrically charged polymer solution or polymer melt [6–10]. Electrospun fibers possess characteristics such as high surface-to-volume ratio, tunable porosity, and flexible morphology with controllable diameter [11], making them suitable for use in wide range of applications. Here, as we discussed above, we primarily aim to exploit the large surface area of electrospun nanofibers in achieving the high absorption capacity.

In literature, cellulosic fibers have been used for absorption of water and other aqueous fluids [12]. However, solvents used for cellulose, such as ionic liquids, are not completely volatile and require coagulation step to get stable fibers [12]. On the other hand, cellulose derivatives such as cellulose acetate, hydroxypropyl cellulose and hydroxypropyl methyl cellulose [11,12], can be easily dissolved in different volatile solvents that makes them suitable for electrospinning. Among these derivatives, cellulose acetate is biocompatible, and a biopolymer which is easily available and has low cost [13]. It shows good hydrolytic stability and can be recycled in the environment by biodegradation [14]. Therefore, we choose cellulose acetate as a material to prepare nanofabric mat for its use as an absorbent core.

In this article, electrospun nanofibers of cellulose acetate, with and without SPA encapsulation, were fabricated and characterized in terms of their surface morphology, mechanical properties, and comfort. To demonstrate their use in female hygiene application, different tests such as free absorbency, equilibrium absorbency, absorbency under load and percentage residue were performed in different mediums, i.e., distilled water, saline solution, and synthetic urine. The results obtained were then compared with some of the known commercially available feminine sanitary napkins.

2. Experimental

2.1. Materials

Cellulose acetate (M_n 29,000) and poly (acrylic acid sodium salt) (M_n 5100) were purchased from Sigma–Aldrich, India. Acetone (99% purity) and N,N-dimethylacetamide (99.5%) were received from Merck India. Distilled water from Millipore was used throughout the experiments. Six feminine hygiene commercial products namely, Whisper Choice, Whisper Ultra Clean, Whisper Maxi-Fit, Whisper Maxi Nights, Stayfree Secure, and Carefree Panty Liner were purchased from the local market.

2.1.1. Commercial feminine sanitary napkins as reference

There are several different types of disposable menstrual pads. They are classified on the basis of their use in different conditions. We have considered six different commercial products (S1–S6) as summarized in Table 1, based on varying vaginal discharge conditions during menstruation cycles.

Table 1

List of commercial feminine hygiene products of various categories considered in this work as reference.

Sample name	Commercial product	Producer	Category	Conditions of use
S1	Whisper Ultra Clean	Procter & Gamble	Ultra-thin	Heavy flow
S2	Whisper Choice Ultra	Procter & Gamble	Regular	Low to medium flow
S3	Stayfree Secure (Regular)	Johnson & Johnson	Regular	Low to medium flow
S4	Whisper Maxi-fit	Procter & Gamble	Maxi/super	Heavy flow
S5	Whisper Maxi nights	Procter & Gamble	Overnight/maternity	Very heavy flow
S6	Carefree Panty Liner	McNeil PPC Inc.	Panty liner	Daily flow

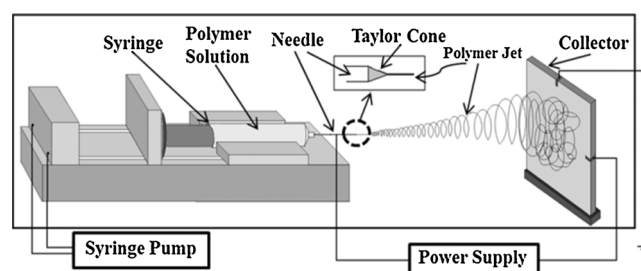


Fig. 1. Schematic of electrospinning setup used in this work.

2.2. Synthetic urine preparation [15]

Synthetic urine was prepared by adding the following to distilled water to give a solution with a final volume of 1 l: 25 g urea, 9 g sodium chloride, 2.5 g sodium phosphate, 3 g ammonium chloride, and 3 g sodium sulfite. Urea (99.5% purity), sodium chloride (99.5% purity), ammonium chloride (AR grade), and sodium sulphite (AR grade) were purchased from SD Fine Chemicals Ltd., Mumbai (India). Sodium phosphate (monobasic anhydrous, 99% purity) was purchased from SRL Pvt. Ltd., Mumbai (India).

2.3. Polymer solution preparation with and without SAP

Cellulose acetate was dissolved in a mixture of acetone and N,N-dimethylacetamide (DMA) (2:1, v:v) to make 16 wt.% solution for electrospinning. The mixture was stirred to get a clear and transparent solution of cellulose acetate. In two other formulations, 5% (w/v) and 10% (w/v) solutions of sodium polyacrylate (SPA) were prepared by mixing SPA in methanol and then added to the above prepared cellulose acetate solution in 1:1 ratio. On adding SPA directly to cellulose acetate solution, it agglomerated and therefore was not recommended for electrospinning.

2.4. Electrospinning

The basic setup of electrospinning consisting of a syringe pump, voltage source, and a collector was purchased from E-spin Nanotech Pvt. Ltd., Kanpur (India). Fig. 1 illustrates the schematic of electrospinning setup and process. Syringe pumps help in maintaining the desired flow rate. When sufficiently high voltage is applied to a liquid droplet, it becomes charged and electrostatic repulsion counteracts the surface tension, resulting in change in shape of the droplet, known as the Taylor cone [10]. At this point, liquid erupts from the surface and fibers are deposited on the grounded collector. Polymer solution gets charged and internal repulsion led to instability in polymer jet, known as Rayleigh instability or whipping motion of the jet, depending on electric field strength [10]. Solvent evaporates in the distance between tip and collector and solidified deposition is obtained on the collector. To get continuous uniform nanofibers or desired morphology, electrospinning parameters were optimized. These were feed rate, voltage applied, tip-to-collector distance and needle (tip) diameter. Table 2 summarizes the final parameters for preparing samples by electrospinning.

Table 2

Process parameters optimized for electrospinning in this work. 'A' represents cellulose acetate solution and 'B' and 'C' represent 5% (w/v) and 10% (w/v) solutions of SPA respectively.

Polymer solution	Applied voltage (kV)	Flow rate ($\mu\text{l}/\text{min}$)	Needle diameter (gauge)	Distance (cm)
A	10	5	18	10
A:B = 1:1	12	10	18	10
A:C = 1:1	12	10	18	10

Besides these, environmental parameters like room temperature (27°C) and relative humidity (60%) were maintained constant for all the experiments.

In this study, three different polymer solutions, i.e., cellulose acetate (CA), cellulose acetate with 5 wt.% SPA (CA5), and cellulose acetate with 10 wt.% SPA (CA10), were used for electrospinning. Aluminum foil placed on the copper collector was used as a substrate to deposit these electrospun fibers.

2.5. Morphological characterization

The surface morphologies of the electrospun nanofibers were observed by using field emission scanning electron microscopy (FESEM) (Model: SUPRA 40, Make: Carl Zeiss, Germany). Electrospun nanofibers were removed from the aluminum foil and cut into small pieces of $1\text{ cm} \times 1\text{ cm}$. All samples were sputtered with thin layer of gold before image analysis in FESEM in order to minimize the charge effect. For commercial products considered as reference, absorbent core was removed and then examined in scanning electron microscope. The average diameter of the nanofibers was measured using ImageJ software considering a minimum of 25 fibers in three different fields of view.

2.6. Specific surface area (SSA) and porosity measurement

The Brunauer–Emmett–Teller (BET) surface area and pore size distribution of electrospun CA nanofibers with and without SPA and two different types of commercial samples were determined by N_2 physisorption using Quantachrome instruments, USA (Model: Autosorb iQ). The weight of the sample was fixed to be 100 mg. All samples were degassed at 80°C for 60 min in nitrogen. The SSAs were determined by a multi-point BET measurement with nitrogen as the adsorbate. Barrett–Joyner–Halenda (BJH) adsorption method was used to determine the pore size distribution.

For determining the porosity, samples were cut in $2\text{ cm} \times 2\text{ cm}$ size and weighed. The thickness of the samples was measured using digital micrometer (Mitutoyo, Japan) at minimum three different places. The apparent volume (V_a) was calculated using the average thickness of sample. The volume of the fibrous mat (V_g) was determined on the basis of cellulose acetate density (1.3 g cm^{-3}) and SPA (0.55 g cm^{-3}) density and their weight ratio. For commercial samples, density of absorbent core was assumed to be 0.5 g cm^{-3} [16]. Finally, the porosity of the sample was determined using the following equation [17]:

$$\text{Porosity} = \left[1 - \left(\frac{V_g}{V_a} \right) \right] \times 100.$$

2.7. Free absorbency test [15]

This test was done to quantify the absorption capacity of sample with respect to time, when allowed to swell freely. Electrospun nanofibers were removed from the aluminum foil to prepare free-standing fabric mat with thickness approximately 0.15 mm, as measured by digital micrometer. Similarly, absorbent core was removed from commercial products. These were then cut into

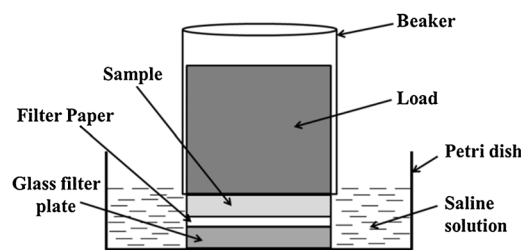


Fig. 2. Test setup used to determine absorbency under load.

approximately $2\text{ cm} \times 2\text{ cm}$ size and weighed, W_1 , i.e., dry weight using microbalance (Model: CPA26P, Make: Sartorius, Germany). The sample was then placed in a beaker containing distilled water and removed after 5 s. The excess water was allowed to drain off with help of tissue paper, for 30 s. The sample was weighed again, W_2 , i.e., wet weight. This process was continued with measurements taken after immersion for 10, 20, 30, 60, 120, and 180 s. Free absorbency can be calculated as:

$$Q = \left[\frac{(W_2 - W_1)}{W_1} \right] \times 100$$

where Q is the percent free absorbency.

Similar procedure was followed to determine the free absorbency with 0.9 wt.% solution of sodium chloride, i.e., saline solution and synthetic urine.

2.8. Equilibrium absorbency [15]

Free absorbency test carried out for time interval of 24 h to know the maximum absorption capacity of the sample is known as equilibrium absorbency. Solutions used are distilled water, saline solution, and synthetic urine. Percentage equilibrium absorbency was calculated as follows:

$$Q' = \left[\frac{(W_2 - W_1)}{W_1} \right] \times 100$$

where Q' is the percent equilibrium absorbency; W_1 is the initial (dry) weight of the sample; W_2 is the final (wet) weight of the sample, after keeping immersed in solution for 24 h.

2.9. Absorbency under load (AUL) [3]

This test was done to know the absorption capacity, if certain load is applied on the sample. By definition, this method is used to measure the ability of a superabsorbent to absorb 0.9 wt.% saline solution against certain pressure. In this study, it is used to measure the absorption capacity of electrospun nanofibers prepared and absorbent core of commercial samples in saline solution, when compressive load is applied while absorption. The setup for AUL tester as shown in Fig. 2 contains a glass filter plate ($d = 30\text{ mm}$), placed in petri dish. A filter paper ($d = 30\text{ mm}$) was placed on top of glass filter plate. Sample was cut in circular shape, with diameter and thickness of 30 and 0.15 mm respectively, and weighed (W_1). Weight, 50 g/cm^2 , was kept on the assembly with help of cylindrical beaker and 0.9 wt.% of NaCl solution was poured in petri dish. Sample was removed after 60 min and weighed (W_2).

Percentage absorbency under load will be given by:

$$Q'' = \left[\frac{(W_2 - W_1)}{W_1} \right] \times 100$$

where Q'' is the percentage absorbency under load; W_1 is the initial (dry) weight of the sample; W_2 is the final (wet) weight of the sample, after immersing in saline solution for 60 min.

All the absorbency tests (free, equilibrium and under load) were conducted under ambient conditions, i.e., room temperature (27 °C) and relative humidity (60%).

2.10. Residue test

This test was conducted to determine the total amount of super-absorbent material, or residue, lost from the fiber matrix after it reaches equilibrium absorption. Samples were cut into small pieces of 2 cm × 2 cm as described in the previous section. Only beaker was weighed as W1. Sample was kept immersed in known amount of distilled water and allowed to reach equilibrium absorbency along with the mechanical shaking for 24 h. Sample was then removed and beaker was placed in the oven (Model: TR60, Make: Nabertherm, Germany) at 110 °C until all water evaporates. It was then weighed (W2) again in order to determine the amount of residue that remained. Residual percentage can be determined by:

$$Y = \left[\frac{(W2 - W1)}{W1} \right] \times 100$$

where Y is the residual percentage.

2.11. Tensile test

Tensile test measures the force required to break a sample specimen and the extent to which the specimen stretches or elongates to that breaking point. Tensile strength was measured with Instron 5948 mechanical tester, USA at the ambient conditions. Electrospun nanofibers mat was peeled off from the aluminum foil and cut into pieces of length (*l*) 6 cm, and breadth (*b*) of 2 cm with thickness of approximately 0.15 mm as measured by digital micrometer. Similarly, the commercial samples as selected for references were cut with same dimensions with thickness varying with the sample. The sample was then placed in-between pneumatic grips and the applied extension rate was 3 mm/min to acquire the stress-strain curve. Similar measurements were performed for these samples under wet conditions (after immersing in DI water for 24 h). Elastic modulus was then measured from the slope of stress-strain curve in the initial linear portion. The use of electrospun CA nanofibers in this work has been demonstrated for feminine hygiene products,

which involves absorption of liquid under pressure causing structural deformation. Therefore, it is important to measure the elastic modulus, which provides information on material's stiffness that is also related to resistance to plastic deformation as well as comfort of the fabric. For each of these measurements, minimum three samples were tested and data were analyzed with *t*-test with significant level, $p < 0.05$, and is presented as mean ± standard deviation.

2.12. Comfort

Comfort of the fabric was quantified in terms of flexural rigidity (bending stiffness) and surface roughness [18,19]. Flexural rigidity is an important parameter for the textile fabrics when used to support load without flexing as is the case here for sanitary napkins. Flexural rigidity can be determined as follows:

$$\text{Flexural rigidity} = E \times I$$

where *E* is the elastic modulus as calculated from tensile testing discussed earlier and *I* is the area moment of inertia given by ($l \times b^3/12$).

Surface roughness (root mean square value) of the fabric was measured using contact profilometer (Model: NanoMap-D, AEP technology, USA) with 1 mg contact force.

3. Results and discussion

3.1. Surface morphology analysis

Surface morphology of absorbent core of selected commercial feminine sanitary napkins was examined using SEM. A representative SEM image of these fibers for sample S1 is shown in Fig. 3a. Feminine sanitary napkins are made up of cellulosic fibers which are found to be in flat-ribbon like shape with width of about 20–50 μm. For sample S1, average diameter was measured to be 28.5 ± 5.7 μm.

Electrospun CA nanofibers as shown in Fig. 3b were long, continuous, and uniform with average diameter 111.9 ± 88.3 nm. Solution of cellulose acetate with 5 wt.% of SPA (CA5) was in suspension and its effect can be observed in the form of partially beaded fibers (Fig. 3c). Number of beaded fibers increased on increasing the SPA concentration to 10 wt.% (CA10) as shown in Fig. 3d. This is

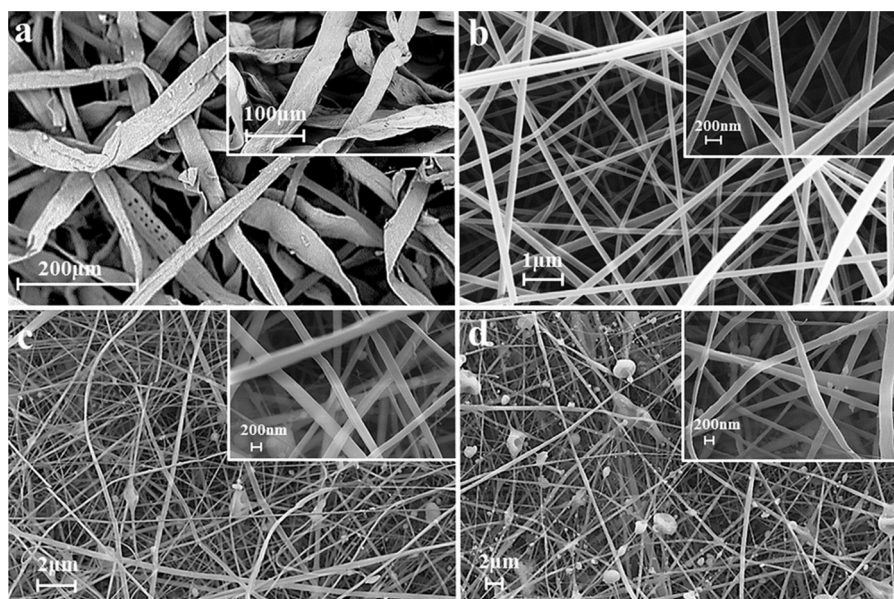


Fig. 3. (a) SEM image of commercial sample S1 and FESEM images of electrospun fibers of (b) CA, (c) CA5 and (d) CA10.

primarily due to suspended solution upon mixing SPA as SPA is sparingly soluble in CA solution. However in both cases, fibers obtained were long and continuous as similar to only CA fibers. Average fiber diameter for both the samples (CA5 and CA10) was measured to be 161.7 ± 98.4 and 181.6 ± 78.5 nm, respectively. Histograms showing the fiber size distribution for CA, CA5 and one of the commercial sample (S1) are shown in Fig. S1. From FESEM image analysis, it is clearly observed that fiber diameter was reduced to more than two orders of magnitude for electrospun fiber samples as synthesized in this work as compared to fabric used in commercial products. We did not observe any significant change in the morphology of these nanofibers except some increase in average fiber diameter (169.2 ± 52.1 nm) after the absorbency tests as discussed later (Fig. S2). This increase in fiber diameter may be due to absorbed water in 24 h.

3.2. Specific surface area and porosity

BET surface area, BJH pore size distribution and porosity data for electrospun nanofiber samples and other commercial samples are summarized in Table 3. BET surface area of electrospun CA nanofibers was found to be $50.21 \text{ m}^2/\text{g}$ which decreased to $22.14 \text{ m}^2/\text{g}$ and $18.36 \text{ m}^2/\text{g}$ when SPA was added as 5 and 10 wt.% respectively. Similarly, total pore volume for electrospun CA nanofibers was found to be $0.174 \text{ cm}^3/\text{g}$, which decreased to 0.168 and $0.146 \text{ cm}^3/\text{g}$ for CA5 and CA10 samples respectively. This decrease in surface area and total pore volume for CA5 and CA10 samples may be attributed mainly due to increased fiber diameter and change in morphology from bead free to beaded fibers on encapsulation of SPA. Surface area of two commercial samples,

Table 3

BET Surface area and porosity values for CA-based nanofiber samples and other commercial samples.

Type of sample	Surface area (m^2/g)	Total pore volume (cm^3/g)	Porosity (%)
CA	50.21	0.174	95.6
CA5	22.14	0.168	94.7
CA10	18.36	0.146	87.8
S1	6.41	0.111	62.1
S4	13.37	0.016	80.8

samples S1 and S4, was measured to be 6.41 and $13.37 \text{ m}^2/\text{g}$, respectively. Total pore volume for these two commercial samples (S1 and S4) was also significantly lower than any CA-based nanofiber samples. Similar trends were observed in porosity measurements. Electrospun CA nanofibers showed the highest porosity (95.6%).

As a summary of surface area and porosity measurement, we observe that surface area, total pore volume and porosity for electrospun CA nanofibers were significantly large compared to any other samples considered.

3.3. Free absorbency

Free absorbency test was done using distilled water, saline solution and synthetic urine to test the absorption capacity of sample. Percent absorbency of electrospun cellulose acetate nanofibers with and without SPA was measured and compared with the selected commercially available feminine sanitary napkins (Fig. 4a–c).

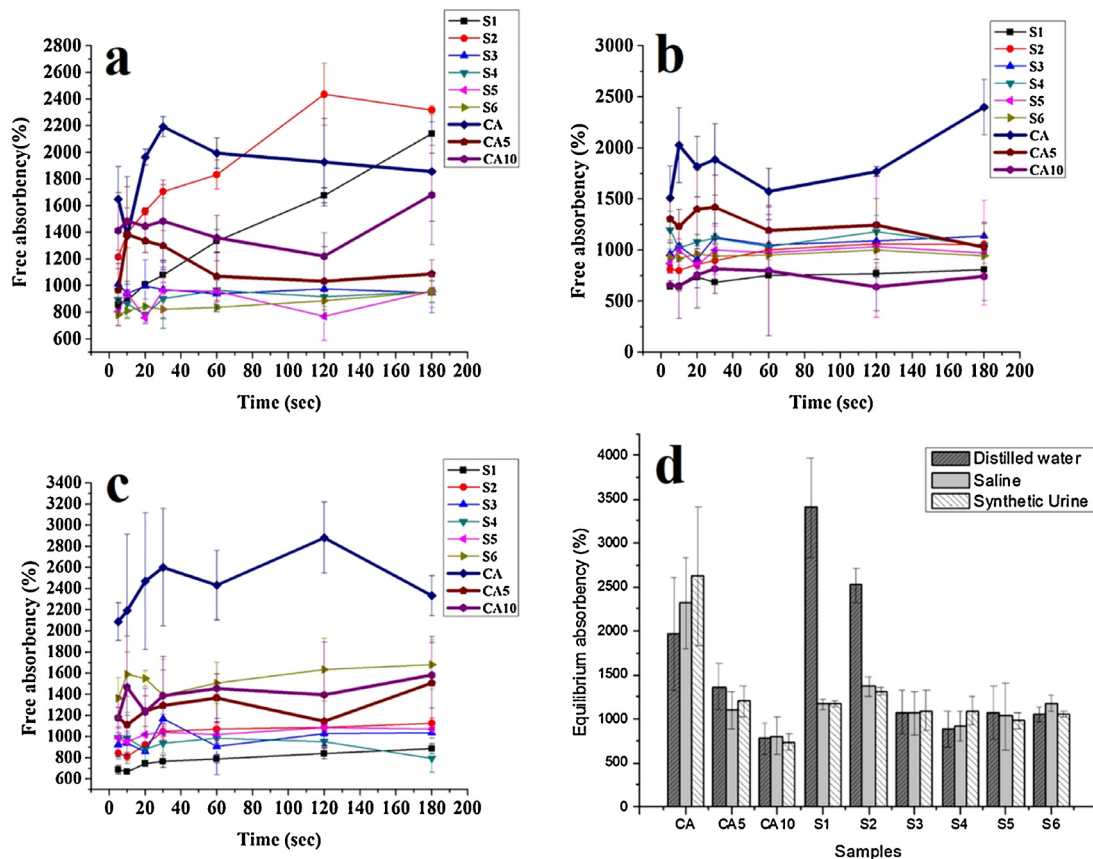


Fig. 4. Free absorbency test in (a) distilled water, (b) saline solution, (c) synthetic urine and (d) equilibrium absorbency for all samples (electrospun nanofibers CA, CA5 and CA10 and all six commercial samples).

Fig. 4a represents the free absorbency results in distilled water. SPA is generally added to increase the absorption capacity and is found to achieve maximum swelling in DI water. However, its encapsulation in nanofibers not only restricts its swelling but interestingly decreases the absorption capacity of CA nanofibers in DI water. For small time span of 20 s, the percent absorbency of CA, CA5, and CA10 nanofibers was measured to be 1963.1, 1336.4 and 1446.9% respectively. This shows that percent absorbency for pure CA nanofibers was 31.9 and 26.3% higher than CA5 and CA10 samples respectively. In spite of increasing the time interval to 180 s, pure CA nanofibers samples had 39.1% and 9.5% more absorbency as compared to CA5 and CA10, respectively. Therefore, CA nanofibers without SPA addition showed maximum percentage free absorbency. When these results were compared with commercial samples taken as reference, in DI water, it was found that the absorption capacity of CA nanofibers for time interval of 20 s was about 48.6, 20.7, 49.2, 60.3, 61.3 and 57.1% higher than samples S1, S2, S3, S4, S5, and S6, respectively. When time interval was increased to 180 s, samples S1 and S2 were found to have 15.3 and 24.9% more absorption capacity as compared to CA nanofibers respectively. However remaining four other commercial samples (S3, S4, S5, and S6) still had nearly 50% less absorbency than pure CA nanofibers.

Although specific composition of commercial samples is not known, but from physical observation, samples S1 and S2 seem to have mainly superabsorbent polymers as their absorbent core; however, S3, S4, S5, and S6 have either no or very less SPA in the combination with some fluffy cellulosic fibers. Thus the absorption in ultra-thin products (S1 and S2) is mainly due to the superabsorbent polymers in their matrix. Therefore, not only the absorption rate but also the overall absorption capacity of S1 and S2 exceeds CA nanofibers when samples were immersed in DI for longer time. On the other hand, other remaining products (S3, S4, S5, and S6) have cellulosic microfiber, and therefore their absorbency was found to be less than pure CA nanofibers primarily due to their lower surface area, pore volume, and porosity compared to CA nanofibers.

Fig. 4b summarizes the absorption capacity of all nine samples in saline solution (0.9 wt.% NaCl). In saline solution also, free absorbency of CA at time interval of 20 s was found to be 23.5 and 58.3% higher than CA5 and CA10, respectively. When this time interval was increased to 180 s, pure CA nanofibers still had about 57.1 and 69.1% higher absorbency than CA5 and CA10 samples. As can be seen from graph (Fig. 4b), the absorption capacity of CA nanofibers was more than all the commercial samples over entire time interval of test. If compared at 180 s, free absorbency of CA was measured to be 66.3, 56.1, 52.6, 56.6, 59.5 and 60.6% more than samples S1, S2, S3, S4, S5, and S6, respectively.

Similar trend was observed for free absorbency in synthetic urine (Fig. 4c). Absorption capacity of pure CA nanofibers for 180 s was 2333.1% which was 35.4 and 32.2% higher than CA5 (1506.7%) and CA10 (1582.1%), respectively. Similarly, pure CA nanofibers were found to have 62, 51.8, 55.6, 65.9, 54.1 and 27.9% more absorbency than S1, S2, S3, S4, S5 and S6 commercial samples respectively at the time interval of 180 s.

Therefore, it is very clear that in saline solution and synthetic urine, the absorption capacity of electrospun CA nanofibers was significantly higher than any of the commercial products and also to CA5 and CA10 nanofiber samples (Fig. 4b and c). In case of DI water also, CA nanofibers showed large absorption capacity as compared to all samples except two commercial samples S1 and S2, which were primarily based on only SAP.

3.4. Equilibrium absorbency

Free absorbency test was extended for time interval of 24 h in all three solutions, i.e., distilled water, saline solution, and synthetic

urine, to find the maximum absorption capacity, also defined as equilibrium absorbency. Fig. 4d illustrates the percentage equilibrium absorbency of electrospun samples and selected commercial samples as references. As observed, equilibrium absorbency of pure CA nanofibers was 30.7 and 60.6% more than CA5 and CA10 samples in DI water. Similarly, it was 52.5 and 65.4% higher in saline solution and 54.1 and 72.1% more in synthetic urine respectively for CA nanofibers as compared to CA5 and CA10 respectively. Therefore, it was observed that absorption capacity for CA nanofibers encapsulated with SPA (CA5 and CA10) was less even after allowing it to swell for 24 h in all three solutions.

Furthermore, while comparing the equilibrium absorbency in DI water with commercial samples, we found that absorbency of S1 and S2 was 73.3 and 28.2% higher than CA samples. This is again because of the swelling of SAPs present in these ultra-thin products (S1 and S2) on increasing the time for immersion in DI water. However for other commercial samples (S3, S4, S5 and S6), equilibrium absorbency in DI water was 45.3, 55.1, 45.6 and 46.45% less than pure CA nanofibers samples owing to their reduced surface area.

Interestingly, the equilibrium absorbency of S1 decreases to about 65.7 and 65.5% in saline solution and synthetic urine respectively while comparing it in DI water. Similarly, for S2 commercial sample, there is a decrease of 45.7 and 47.8% in saline solution and synthetic urine respectively as compared to absorbency in DI water. This behavior can be explained as follows: SPA at molecular structure contains sodium carboxylate groups on the main chain. Sodium gets detached from the chain, leaving only carboxyl ions, when it comes in contact with water [2]. This allows the sodium ions to move freely within the network, which contributes to the osmotic pressure within the gel. The mobile positive sodium ions however cannot leave the gel because they are still weakly attracted to the negative carboxylate ions along the polymer. So the driving force for swelling is the difference between the osmotic pressure inside and outside the gel. Increase in the level of sodium ions outside of the gel will lower the osmotic pressure and reduce the swelling capacity of the gel [20]. This swelling mechanism of SPA explains the sudden decrease in the equilibrium absorbency of commercial sanitary napkins (S1 and S2) in both saline solution and synthetic urine.

From the free absorbency and equilibrium absorbency results, it can be concluded that the electrospun CA nanofibers have significantly large absorption capacity for saline solution and synthetic urine as compared to the commercial products in all the categories of use. Even in recent literature based on cellulose-based fiber materials [12], absorbency values reported for untreated cellulose-based fibers except bacterial cellulose were significantly low as

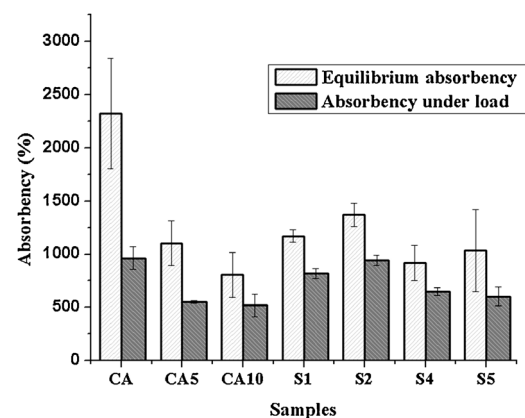


Fig. 5. Absorbency under load in saline solution for different electrospun nanofibers samples and selected commercial samples.

compared to what we reported here (Table S1). This is primarily due to the fact that all these cellulose fibers reported are in micron size as similar to commercial samples. More interestingly, the encapsulation of SPA in these CA nanofibers (CA5 and CA10) is rather decreasing the absorption capacity of nanofibers even when allowed to swell freely for 24 h. Therefore, it is very clear that use of SPA in CA nanofibers does not facilitate in enhancing the absorption efficiency of the matrix.

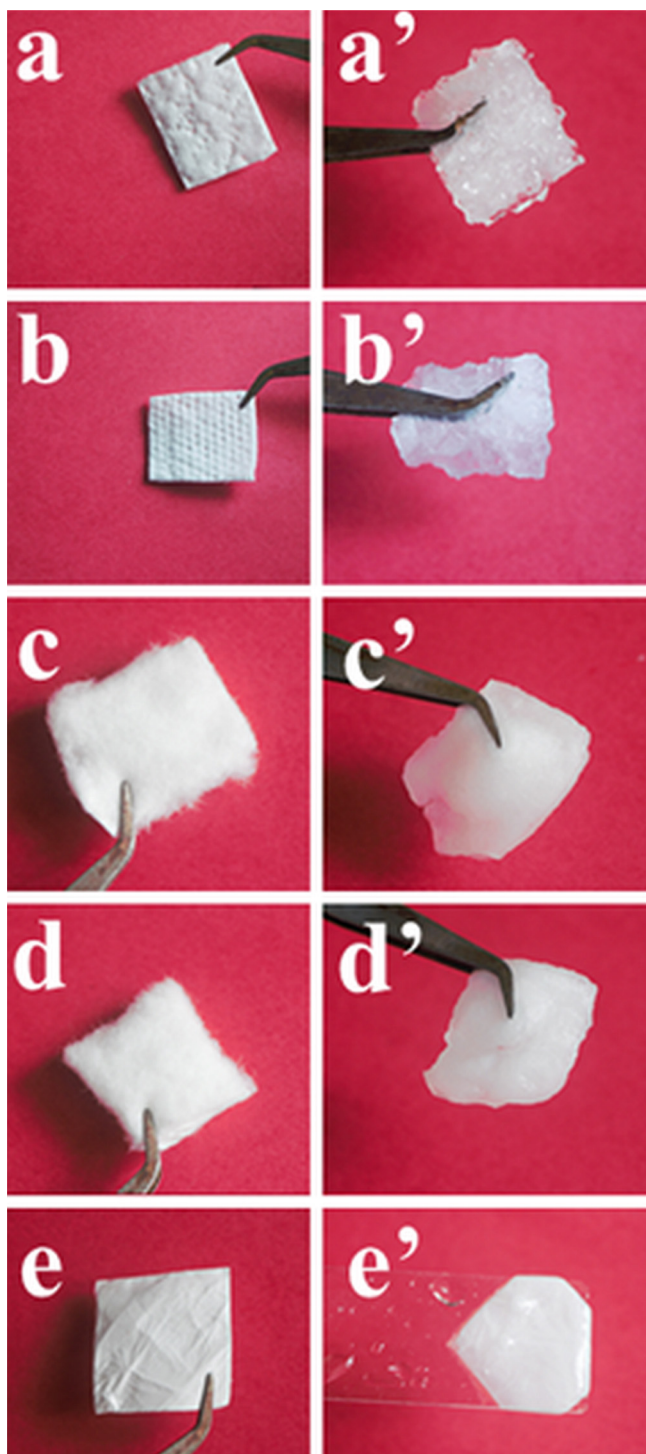


Fig. 6. Pictorial representation of the absorbent cores of commercial samples (a) S1, (b) S2, (c) S5, (d) S4 and (e) electrospun CA nanofibers. a'–e' shows the changes after dipping in distilled water for 10 min for respective samples.

3.5. Absorbency under load (AUL)

This test measures the effect of mechanical compression on the swelling process of sample and is an important consideration for the proposed use of CA nanofibers for feminine hygiene applications. The compressive load applied on the sample changes the shape of the sample and may alter the surface properties like suppressing the internal structure. As a result, there is decrease in the absorbency under load compared to the free swelling, i.e., equilibrium absorbency in saline solution as shown in Fig. 5. Absorbency under load for electrospun CA nanofibers was measured to be 961.9%, which was reduced to 550.1 and 517.7% for CA5 and CA10, respectively. This means that CA nanofibers have 42.8 and 46.2% more absorbency under load than CA5 and CA10 respectively. Similarly, absorbency under load for pure CA nanofiber was found to be 15.1, 2.2, 32.8 and 37.5% more than S1, S2, S4 and S5 samples respectively. These results also confirm that CA nanofibers exhibited much improved performance as compared to any other samples including all commercial samples.

3.6. Residue test

The amount of losses from the matrix was quantified by using residue test. The cellulosic fibers or loosely held SAP granules in commercial samples mainly contribute toward the residue from absorbent core. Fig. 6 represents the structure of absorbent core of commercial samples and CA nanofibers before (Fig. 6a–e) and after dipping in distilled water (Fig. 6a'–e') for 10 min. SAP granules swell upon absorbing liquid and form a liquid impermeable wall of gel and inhibit further movement of liquid. Therefore, these polymers are randomly distributed within the absorbent core [2]. Smaller SAP granules increase the absorption rate because of increase in the surface area, but they have tendency to fall out of the matrix, therefore contributing toward the residue as shown in Fig. 6a' and b', whereas in some other cases, loosely held cellulosic fibers in the absorbent core contribute to the residue (Fig. 6c' and d'). However importantly there is no major structural change in CA nanofibers except little shrinkage (Fig. 6e') as compared to commercial samples.

Quantitative results of residue tests are summarized in Fig. 7. Electrospun nanofibers of pure CA and with SPA (CA5 and CA10) have almost negligible residue compared to the feminine sanitary napkins, S1 ($0.11 \pm 0.05\%$) and S2 ($0.34 \pm 0.12\%$), respectively. This observation also confirms the incorporation of SPA in the form of beads in nanofibers as if it is loosely held within nanofiber matrix, and one may expect a significant amount of loss of SPA after residue test similar to commercial samples. For other commercial samples S3, S4, S5 and S6, whole cellulosic fiber matrix disintegrates due to mechanical shaking for 24 h done along with

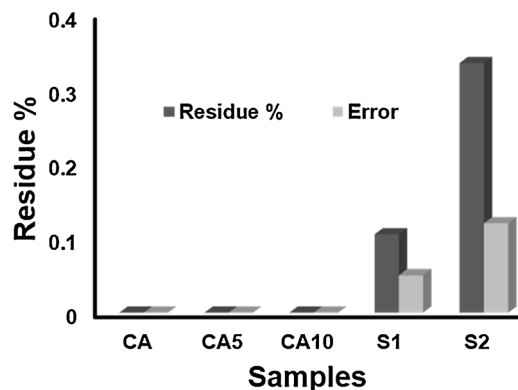


Fig. 7. Residue test for electrospun fiber samples (CA, CA5 and CA10) and commercial samples (S1 and S2).

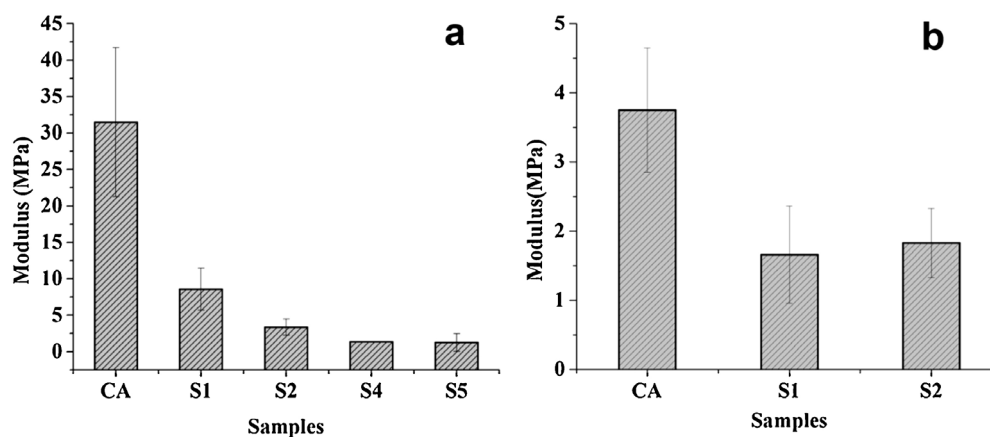


Fig. 8. Young's modulus for different samples (electrospun CA nanofibers and commercial samples) under (a) dry and (b) wet (after keeping immersed in DI water for 24 h) conditions.

equilibrium absorbency. Therefore entire initial weight of samples acts as residue and thus not compared in Fig. 7. The electrospun CA nanofibers are strongly entangled and therefore do not contribute to any residue. The same was true after encapsulating with SAP (CA5 and CA10).

3.7. Tensile test

The inadequate tensile strength of absorbent core may lead to its breakage or tearing which may result in the leakage of fluid thereby decreasing the product's efficiency. Therefore, mechanical properties (elastic modulus, breaking strength and elongation under dry and wet conditions) of electrospun CA-based nanofibers were measured and compared with other commercial samples. These results are represented in Fig. 8 and Table S2. Original stress-strain curves used to calculate the modulus of elasticity are added as supporting information (Fig. S3). There is a significant difference between the elastic modulus of electrospun CA based nanofibers and commercial samples. Under dry conditions, for S1, S2, S4, and S5, the modulus are 8.6 ± 2.9 , 3.4 ± 1.1 , 1.4 ± 0.1 and 1.3 ± 1.2 MPa respectively while for CA nanofibers, modulus of elasticity was found to be 31.5 ± 10.2 MPa (Fig. 8a). There was no significant change in modulus of elasticity for CA5 (31.3 ± 8.9 MPa) and CA10 (29.8 ± 5.5 MPa) as compared to only CA nanofibers sample. The absorbent core of commercial samples (S1, S2, S4 and S5) is mainly made by loosely held cellulosic fibers and strength is provided by using different layers, above and below the core. However higher elastic modulus values for electrospun CA nanofibers which are in the form of non-woven matrix may be explained by the compact structure and entanglement of nanofibers leading to the confinement of supramolecular structures [21]. Similar observations are made for these samples under wet conditions as shown in Fig. 8b. Commercial samples (S4 and S5) were disintegrated under wet conditions and therefore could not be tested. These results show that mechanical strength of pure CA nanofibers was more than any other commercially available samples and thus directly can be used as absorbent core in female hygiene products.

3.8. Comfort

The flexural rigidity (bending stiffness) for CA, CA5 and CA10 nanofabric was measured to be 1.26, 1.25 and 1.19 N m^2 respectively. For commercial samples S1, S2, S4 and S5, flexural rigidity values were 0.34, 0.14, 0.06 and 0.05 N m^2 respectively. We can clearly observe that for CA-based nanofabric (CA, CA5 and CA10), ability to absorb load without flex is significantly higher.

Further, surface roughness 3D data for different fabrics are shown in Fig. S4. The root mean square roughness for CA nanofabric was measured to be $3.84 \mu\text{m}$ which was least among other samples ($5.18 \mu\text{m}$ for CA5 fabric and $11.93 \mu\text{m}$ for commercial sample, S1).

Higher value of flexural rigidity and lower surface roughness for CA nanofibers sample make them more comfortable even as compared to commercial samples and therefore can be potentially used in feminine hygiene applications.

4. Conclusions

CA electrospun nanofibers were fabricated with and without encapsulating different amount of SPA into their fiber matrix and we successfully demonstrated their application in feminine hygiene products. Free absorbency, equilibrium absorbency and absorbency under load were carried out in three different mediums (DI water, saline solution, and synthetic urine) for all samples fabricated in this work and results were compared further with a wide variety of commercially available female sanitary napkins used for various stages during female menstrual cycles. In case of DI water, CA nanofibers performed significantly better than two other nanofibers samples encapsulated with SPA and also outperformed most of these commercial samples used for reference. Only in case of free absorbency and equilibrium absorbency in DI water, two commercial samples (S1 and S4) which were primarily based on SAP only, showed more absorbency than CA electrospun nanofibers. However more importantly, only CA electrospun nanofibers showed significantly large absorbency in all conditions as compared to any other fabricated as well as commercial samples in saline solution and synthetic urine solutions.

Equally important, residual percentage for all electrospun nanofiber samples (CA, CA5 and CA10) was found to be negligible. Furthermore, mechanical strength and comfort were also found to be more for electrospun CA nanofibers as compared to SPA encapsulated nanofibers and commercial samples.

Most importantly, we found that loading of SPA in CA nanofibers not only decreased the surface area and porosity but also restricted SPA to swell resulting in decreased absorption capacity than only CA nanofibers. This clearly suggests that use of SPA (or in general SAPs) can be eliminated if CA nanofibers are used to make the absorbent core in feminine sanitary napkins without compromising with the absorption efficiency. This will not only reduce the health related risks such as toxic shock syndrome linked with the use of SAPs but also make the disposable female sanitary napkin products more environmental friendly, as SAPs are generally non-biodegradable.

Acknowledgements

CSS acknowledges the financial support received from DST in the form of INSPIRE Faculty Award research grant. Authors also acknowledge Indian Institute of Technology Hyderabad in procur-ing state of the art research facilities used to carry out this work. We would like to express our thanks to Anand Kumar for his help in FESEM imaging and BET measurements. CSS also acknowledges the useful discussions with Dr. Mudrika Khandelwal.

Appendix A. Supplementary data

Supplementary data associated with this article can be found, in the online version, at [doi:10.1016/j.apmt.2016.07.002](https://doi.org/10.1016/j.apmt.2016.07.002).

References

- [1] R. Garg, S. Goyal, S. Gupta, India moves towards menstrual hygiene: subsidized sanitary napkins for rural adolescent girls—issues and challenges, *Matern. Child Health J.* 16 (2012) 767–774.
- [2] D. Das, Composite nonwovens in absorbent hygiene products, in: D. Das, B. Pourdeyhimi (Eds.), *Composite Nonwoven Materials*, Woodhead Publishing, UK, 2014, pp. 74–88.
- [3] J.Z. Mohammad, K. Kourosh, Superabsorbent polymer materials: a review, *Iran. Polym. J.* 17 (2008) 451–477.
- [4] K.S. Kumar, Is Your Sanitary Napkin Safe, *The New Indian Express*, August 28, 2013 <http://www.newindianexpress.com/cities/bangalore/is-your-sanitary-napkin-safe/2013/08/28/article1755252.ece>.
- [5] S.F. Berkley, A.W. Hightower, C.V. Broome, A.L. Reingold, The relationship of tampon characteristics to menstrual toxic shock syndrome, *J. Am. Med. Assoc.* 258 (1987) 917–920.
- [6] S. Ramakrishna, K. Fujihara, T.W. Eong, T. Lim, Z. Ma, *An Introduction to Electrospinning and Nanofibers*, World Scientific Publishing Co. Pte. Ltd., Singapore, 2005.
- [7] B. Cramariuc, R. Cramariuc, R. Scarlet, L.R. Manea, I.G. Lupu, O. Cramariuc, Fiber diameter in electrospinning process, *J. Electrostat.* 71 (2013) 189–198.
- [8] Formhals, A. Process and Apparatus for Preparing Artificial Threads. US. Patent 1,975,504, October 2, 1934.
- [9] J. Doshi, D.H. Reneker, Electrospinning process and applications of electrospun fibers, *J. Electrostat.* 35 (1995) 151–160.
- [10] Z.M. Huang, Y.Z. Zhang, M. Kotaki, S. Ramakrishna, A review on polymer nanofibers by electrospinning and their applications in nanocomposites, *Compos. Sci. Technol.* 63 (2003) 2223–2253.
- [11] M.W. Frey, Electrospinning cellulose and cellulose derivatives, *J. Macromol. Sci. Polym. Rev.* 48 (2008) 378–391.
- [12] M.A. Hubbe, A. Ayoub, J.S. Daystar, R.A. Venditti, J.J. Pawlak, Enhanced absorbent products incorporating cellulose and its derivatives: a review, *BioResources* 8 (2013) 6556–6629.
- [13] R. Konwarh, N. Karak, M. Misra, Electrospun cellulose acetate nanofibers: the present status and gamut of biotechnological applications, *Biotechnol. Adv.* 31 (2013) 421–437.
- [14] W. Zhou, J. He, S. Cui, W. Gao, Studies of electrospun cellulose acetate nanofibrous membranes, *Open Mater. Sci. J.* 5 (2011) 51–55.
- [15] M. Frazier, *Superabsorbent Nanofiber Matrices* (Ph.D. Thesis), The University of Akron, OH, USA, 2006.
- [16] S. Bernal, R. Bentley, P. Crane, J. Davis, N. Malakouti, Absorbent core structures having undulations. Patent Application WO2006099112, September 21, 2006.
- [17] D.C. Aduba Jr., J.A. Hammer, Q. Yuan, W.A. Yeudall, G.L. Bowlin, H. Yang, Semi-interpenetrating network (sIPN) gelatin nanofiber scaffolds for oral mucosal drug delivery, *Acta Biomater.* 9 (2013) 6576–6584.
- [18] S. Kawabata, M. Niwa, Fabric performance in clothing and clothing manufacture, *J. Text. Inst.* 80 (1989) 19–50.
- [19] A. Gupta, Design of an Absorbent and Comfortable Sanitary Napkin for Applications in Developing Countries (B.Sc. Thesis), Massachusetts Institute of Technology, 2014, June.
- [20] M. Elliott, *Superabsorbent Polymers*, BASF Aktiengesellschaft, Ludwigshafen, Germany, 2004.
- [21] A. Arinstein, M. Burman, O. Gendelman, E. Zussman, Effect of supramolecular structure on polymer nanofiber elasticity, *Nat. Nanotechnol.* 2 (2007) 59–62.